J. Cent. South Univ. (2015) 22: 2287−2296
DOI: 10.1007/s11771-015-2753-x

Springer

Experimental investigation of axially loaded steel fiber reinforced high strength concrete-filled steel tube columns

LU Yi-yan(卢亦焱), LI Na(李娜), LI Shan(李杉), LIANG Hong-jun(梁鸿骏)

School of Civil Engineering, Wuhan University, Wuhan 430072, China

Abstract: An experimental study on the compressive behavior of steel fiber reinforced concrete-filled steel tube columns is presented. Specimens were tested to investigate the effects of the concrete strength, the thickness of steel tube and the steel fiber volume fraction on the ultimate strength and the ductility. The experimental results indicate that the addition of steel fibers in concrete can significantly improve the ductility and the energy dissipation capacity of the concrete-filled steel tube columns and delay the local buckling of the steel tube, but has no obvious effect on the failure mode. It has also been found that the addition of steel fibers is a more effective method than using thicker steel tube in enhancing the ductility, and more advantageous in the case of higher strength concrete. An analytical model to estimate the load capacity is proposed for steel tube columns filled with both plain concrete and steel fiber reinforced concrete. The predicted results are in good agreement with the experimental ones obtained in this work and literatures.

Key words: concrete-filled steel tube (CFST) columns; steel fiber; high strength concrete; axial load; ductility; load capacity

1 Introduction

Concrete-filled steel tube (CFST) columns have been widely used due to their high load capacity, stiffness, ductility and fire resistance. With the advances in technology, high strength concrete has become a feasible alternative to normal strength concrete in tall buildings. However, the use of high strength concrete, characterized by a brittle failure, reduces the deformation capacity and has an adverse effect on the post-peak behavior of CFST columns [1−2].

LIU and GHO [3] and ZEGHICHE and CHAOUI [4] demonstrated that it is possible to use high strength concrete to achieve ductile behavior. The ductility of the CFST columns can be improved by confining the concrete within a tube with high strength or small diameter-to-thickness ratio [5], which is certain to increase the construction cost. ZHANG and WANG [6] stated that the inherent brittleness of high strength concrete plays an important role in the behavior of the CFST columns. An obvious shear deformation may occur in the high strength concrete core under axial compression, which results in an uneven distribution of confinement and aggravates the local buckling of the steel tube. Therefore, the CFST columns exhibit a sharp drop of axial load after the peak load and fail with a shear mode. TAO et al [7] concluded that adding steel fibers into concrete is an effective and economic way in enhancing the ductility of the stub CFST columns with square cross section. This is because that adding fibers into concrete brings about the advantages including elimination of concrete cracks at early stage, reduction of concrete plastic cracks with improved post-peak behavior and greater flexural and tensile strengths [8−9].

The use of fiber reinforced concrete (FRC) with low and normal strength instead of plain concrete (PC) as infill in CFST columns has been investigated by CAMPIONE et al [10], ELLOBODY and GHAZY [11−12], TAO et al [13], GOPAL and MANOHARAN [14] and KODUR and LIE [15]. In these studies, the CFST columns were of slender column or/and tested under eccentric load. The enhanced flexural and tensile strengths of fiber reinforced concrete were applied to ease the increasing strain gradient associated with increasing flexure. Therefore, some beneficial effects of composite behavior in terms of strength are obtained. In addition, the presence of steel fibers provides a higher stiffness, which delays the increasing of lateral deflection, and then enhances the ductility and energy dissipation capacity of CFST columns.

With the increasing use of high strength concrete in modern buildings, the addition of steel fibers is expected to be an effective method in improving the behavior of

Foundation item: Project(51078294) supported by the National Natural Science Foundation of China; Project(201101411100025) supported by the Doctoral Fund of Ministry of Education of China
Received date: 2014−04−15; **Accepted date:** 2014−06−15
Corresponding author: LI Na, PhD Cansicate; Tel: +86−27−68775832; E-mail: ln950228@163.com

the steel tube columns filled with high strength concrete. Like the above mentioned studies, the existing studies focus on the beneficial effects of the enhanced tensile and flexural strengths and stiffness compared with plain concrete. TOKGOZ and DUNDAR [16] studied the effect of steel fiber on the behavior of eccentrically loaded slender rectangular CFST columns. The result indicates that the use of FRC improves the ductility and deformation capacity, but has little effect on the ultimate strength. PORTOLES et al [17] reported an experimental investigation on the structural behavior of eccentrically loaded slender steel tube columns filled with normal, high and ultra-high strength concrete. The infills included PC, FRC and bar reinforced concrete (BRC). The results showed that in the case of normal strength concrete, the steel tube columns filled with FRC exhibit better performance than the steel tube columns filled with PC and perform similarly to the steel tube columns filled with BRC. However, because the global behavior predominates over the section behavior for slender CFST columns, adding steel fibers does not help in the case of high and ultra-high strength concrete.

Few researchers have investigated the enhancing effects of steel fiber on the short and stub steel tube columns with high strength concrete [7, 18]. On the other hand, the length-to-diameter ratio of low story columns in high-rise buildings is relative small, and these columns with high strength concrete are more susceptible to a brittle shear failure [19]. In this work, experimental tests were conducted to investigate the shear reinforcing effect of steel fibers on short steel tube columns filled with high strength concrete. Specifically, 36 specimens, including 9 plain concrete-filled steel tube (PCFST) specimens and 27 steel fiber reinforced concrete-filled steel tube (SFRCFST) specimens, were tested under axial load. The axial load−axial shortening relationships were measured from the tests. The ultimate strengths and the failure modes were also obtained from the tests. The effects of the concrete strength, the thickness of steel tube and the steel fiber volume fraction on the ultimate strength and the ductility were discussed. Furthermore, an analytical model was proposed to calculate the load capacity of the steel tube columns filled with both plain concrete and steel fiber reinforced concrete.

2 Experimental programs

2.1 Test specimens

Thirty-six CFST specimens, including 9 PCFST specimens and 27 SFRCFST specimens, were tested under axial load. The tested parameters were concrete strength f_{cu}, thickness of steel tube t, and steel fiber volume fraction V_f. All specimens had a length (L) to diameter (D) ratio of 3. The details of all specimens are summarized in Table 1, in which the three terms of label C××-××-×× represent the concrete strength, the thickness of steel tube and steel fiber volume fraction times 100, respectively. Each group (C××-××) includes four specimens with the same thickness of steel tube and concrete strength, but different steel fiber volume fractions.

2.2 Material properties

The steel frameworks of all specimens were fabricated from seamless circular steel tubes. The average values of yield strength f_y and elastic modulus E_s of the steel tube determined from coupon tests were 306 MPa and 205 GPa, respectively. Three different concrete strength grades were considered in this work. Self-consolidating concrete was applied to achieve a uniform distribution of steel fibers throughout the concrete. The plain concrete mix, the slump flow and the cube strength are listed in Table 2. The steel fiber employed was the hooked-end type with length L_f = 30 mm and diameter d=0.52 mm. The tensile strength of the fiber, as provided by the manufacturer, was larger than 1060 MPa. The slump flows of steel fiber reinforced concrete (SFRC) were all larger than 550 mm. The compressive strengths of the SFRC at 28 days are summarized in Table 1.

2.3 Specimen preparation

A stiffened end cap of 10 mm was attached at the base of each steel tube, and then the concrete was filled without any vibration. The specimens were left to cure in the laboratory for 28 days. Prior to testing, the top surface of concrete core was roughened with a wire brush, and then a thin layer of high strength cement was poured on the roughened surface. This procedure was adopted to minimize the effect of concrete shrinkage so that the steel tube and the concrete core can be loaded simultaneously during testing.

2.4 Test setup and instrumentation

The tests were conducted using a universal testing machine with a capacity of 5000 kN. The test arrangements for the specimens are shown in Fig. 1(a). The load was applied in an increment of 50 kN before peak load. Each load interval was maintained for 2−3 min. The load was slowly applied near and after the peak load to investigate the post-peak behavior of the specimens.

Four linear variable differential transducers (LVDTs) were located vertically to measure the axial shortenings. Strain gauges were placed on the exterior of the steel tubes to measure the vertical deformations and perimeter expansions. The layout of the LVDTs and strain gauges are shown in Fig. 1(b).

Table 1 Specimen properties and test results

Group	Specimen	D/mm×t/mm× L/mm	f_y/MPa	f_{cu}/MPa	θ	V_f/%	δ_u/mm	δ_{85}/δ_u	E/(kN·mm)	N_u/kN	SI	λ	N_c/kN	N_c/N_u
C50-3	C50-3-0	129 × 3 × 387	306	53.7	0.71	0	2.51	2.13	4418	1068	1.22	0.54	1074	1.01
	C50-3-0.6	129 × 3 × 387	306	55.3	0.69	0.6	2.48	2.29	5075	1093	1.23	0.60	1077	0.99
	C50-3-0.9	129 × 3 × 387	306	56.3	0.68	0.9	2.41	2.83	6542	1118	1.24	0.67	1139	1.02
	C50-3-1.2	129 × 3 × 387	306	58.8	0.65	1.2	2.84	3.20	8902	1162	1.26	0.79	1157	1.00
C50-4	C50-4-0	131 × 4 × 393	306	53.7	0.95	0	3.24	2.18	7289	1280	1.28	0.58	1264	0.99
	C50-4-0.6	131 × 4 × 393	306	55.3	0.93	0.6	2.86	2.60	8373	1360	1.34	0.74	1269	0.93
	C50-4-0.9	131 × 4 × 393	306	56.3	0.91	0.9	2.61	2.92	9130	1403	1.37	0.83	1351	0.96
	C50-4-1.2	131 × 4 × 393	306	58.8	0.87	1.2	3.17	3.36	13518	1459	1.39	0.94	1375	0.94
C50-5	C50-5-0	133 × 5 × 399	306	53.7	1.20	0	2.97	2.21	7818	1454	1.29	0.53	1456	1.00
	C50-5-0.6	133 × 5 × 399	306	55.3	1.17	0.6	2.88	2.94	9941	1470	1.29	0.56	1461	0.99
	C50-5-0.9	133 × 5 × 399	306	56.3	1.15	0.9	2.96	3.01	13060	1518	1.32	0.64	1564	1.03
	C50-5-1.2	133 × 5 × 399	306	58.8	1.10	1.2	2.64	3.99	16550	1569	1.34	0.77	1594	1.00
C60-3	C60-3-0	129 × 3 × 387	306	60.9	0.63	0	2.31	2.07	4032	1095	1.16	0.43	1142	1.04
	C60-3-0.6	129 × 3 × 387	306	62.4	0.61	0.6	2.67	2.12	5177	1128	1.18	0.51	1146	1.02
	C60-3-0.9	129 × 3 × 387	306	64.0	0.60	0.9	2.52	3.24	7782	1147	1.18	0.56	1208	1.05
	C60-3-1.2	129 × 3 × 387	306	66.2	0.58	1.2	2.17	4.33	10715	1192	1.20	0.69	1226	1.03
C60-4	C60-4-0	131 × 4 × 393	306	60.9	0.84	0	3.52	2.17	8618	1320	1.24	0.52	1333	1.01
	C60-4-0.6	131 × 4 × 393	306	62.4	0.82	0.6	2.52	2.71	11843	1389	1.28	0.66	1337	0.96
	C60-4-0.9	131 × 4 × 393	306	64.0	0.80	0.9	2.63	3.56	18839	1430	1.30	0.74	1419	0.99
	C60-4-1.2	131 × 4 × 393	306	66.2	0.78	1.2	2.83	4.12	21466	1452	1.30	0.79	1443	0.99
C60-5	C60-5-0	133 × 5 × 399	306	60.9	1.06	0	2.76	2.08	6900	1548	1.30	0.58	1524	0.98
	C60-5-0.6	133 × 5 × 399	306	62.4	1.03	0.6	3.15	2.40	9165	1581	1.31	0.63	1530	0.97
	C60-5-0.9	133 × 5 × 399	306	64.0	1.01	0.9	2.97	3.41	13396	1609	1.32	0.68	1632	1.01
	C60-5-1.2	133 × 5 × 399	306	66.2	0.98	1.2	3.17	3.85	22096	1661	1.34	0.76	1662	1.00
C70-3	C70-3-0	129 × 3 × 387	306	69.7	0.55	0	2.28	2.04	6444	1266	1.23	0.66	1226	0.97
	C70-3-0.6	129 × 3 × 387	306	71.6	0.53	0.6	3.58	2.36	8439	1287	1.23	0.72	1229	0.96
	C70-3-0.9	129 × 3 × 387	306	74.6	0.51	0.9	3.26	2.91	10686	1301	1.21	0.85	1291	0.97
	C70-3-1.2	129 × 3 × 387	306	76.4	0.50	1.2	2.70	4.54	17999	1356	1.24	0.91	1309	0.97
C70-4	C70-4-0	131 × 4 × 393	306	69.7	0.74	0	3.46	2.45	8762	1469	1.28	0.65	1416	0.96
	C70-4-0.6	131 × 4 × 393	306	71.6	0.72	0.6	2.17	3.61	9746	1482	1.27	0.68	1421	0.96
	C70-4-0.9	131 × 4 × 393	306	74.6	0.69	0.9	2.48	3.78	13609	1496	1.25	0.71	1503	1.00
	C70-4-1.2	131 × 4 × 393	306	76.4	0.67	1.2	2.01	4.95	17158	1542	1.27	0.80	1527	0.99
C70-5	C70-5-0	133 × 5 × 399	306	69.7	0.93	0	2.52	2.05	6320	1659	1.30	0.62	1608	0.97
	C70-5-0.6	133 × 5 × 399	306	71.6	0.90	0.6	2.04	2.96	8316	1673	1.29	0.64	1613	0.96
	C70-5-0.9	133 × 5 × 399	306	74.6	0.87	0.9	2.02	3.61	12180	1712	1.29	0.73	1716	1.00
	C70-5-1.2	133 × 5 × 399	306	76.4	0.85	1.2	2.62	4.36	17320	1774	1.32	0.81	1746	0.98

Table 2 Parameters for plain concrete

Mix ID	Cement/(kg·m^{-3})							Slump flow/mm	Cubic concrete strength/MPa
	Cement	Fly ash	Silica fume	Water	Sand	Gravel	Super-plasticizer		
C50	335.5	132	27.5	189.9	747.1	856	3.3	672	53.7
C60	366	144	30	177.1	730.3	836.8	4.8	648	60.9
C70	366	144	30	163.3	736.5	843.9	7.8	645	69.7

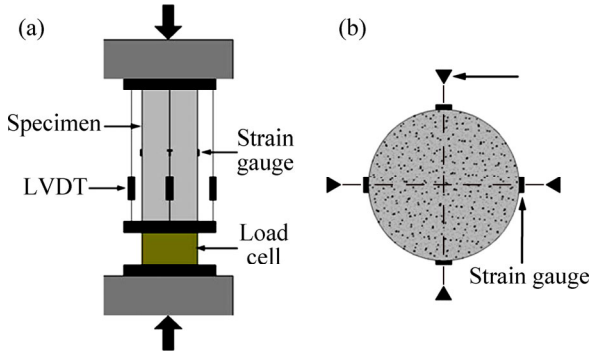

Fig. 1 Test arrangement (a) and layout (b) of instrumentations

3 Experimental results and discussion

3.1 Failure modes and axial load−strain curves

The PCFST specimens present shear failure of the concrete core. After the external steel tube is removed, an obvious shear failure plane is found to exist among the bulges, as shown in Fig. 2. The axial load drop is associated with the formation of the major diagonal crack inside the concrete core. The friction between the surfaces of the cracked concrete is believed to be the main mechanism that maintains the resistance to the applied axial load.

Fig. 2 Shear failure plane in concrete core

The failure mode of the SFRCFST specimens is similar to that of the PCFST specimens. The cracked surfaces slide against each other as the axial load increases. However, the presence of the SFRC delays the bulge formation of the steel tube. This is because that the confinement from the steel fibers relieves the concrete expansion pressures on the exterior steel tube when the concrete cracks. In addition, the SFRCFST specimens exhibit a more moderate drop of the axial load. This may be due to the bridging effect of the steel fibers crossing the concrete cracks, which helps to maintain the resistance to the axial load.

The axial load versus transverse strain responses of steel tube for some specimens are shown in Fig. 3. Figure 3(a) shows the variation of transverse strain of steel tube for the SFRCFST and PCFST specimens during loading. Steel fiber has no effect on the transverse strain of steel tube when the applied load is relatively small. However, when the applied load increases to a certain level, the transverse strain of PCFST specimens increases with a much higher rate than the corresponding SFRCFST specimens. This is because that the steel fibers control the development of concrete crack, and delay the lateral expansion of concrete. It is worth noting that the transverse strain of steel tube at the maximum load

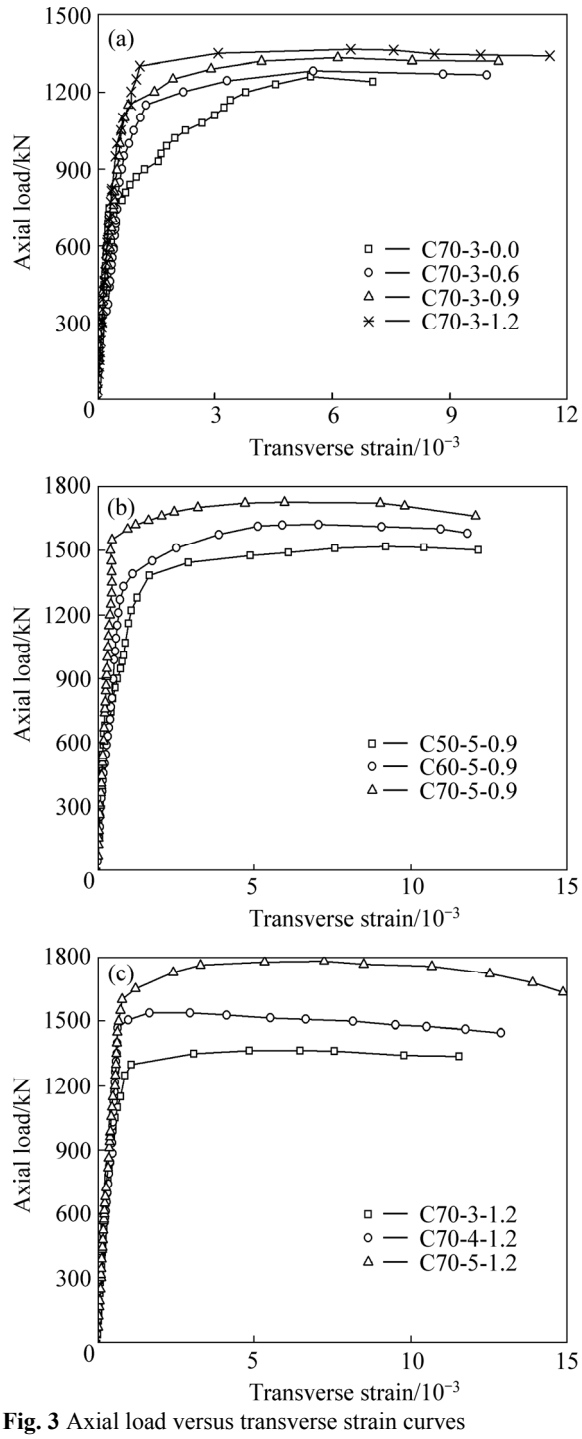

Fig. 3 Axial load versus transverse strain curves

increases with steel fiber volume fraction.

Figure 3(b) demonstrates the effects of concrete strength on axial load–transverse strain curves. Due to the reduced deformability of the higher strength concrete, the transverse strain of steel tube is smaller for the specimens with higher strength concrete and a decreased transverse strain of steel tube at the maximum strain.

Figure 3(c) shows the axial load–transverse strain relationships for the SFRCFST specimens with different thicknesses of steel tube. Increasing the thickness of steel tube has no obvious effect on the transverse strain of steel tube.

3.2 Axial load−axial shortening curves

The ultimate strengths N_u are listed in Table 1. When the concrete strength increases, the ultimate strength of the SFRCFST specimens increases. When the thickness of steel tube increases, so does the ultimate strength. The axial load–axial shortening curves of some specimens are shown in Figs. 4–6. It is seen that, yield load is the applied load at which the slope of coefficient of the axial load–axial shortening curve decreases, that is, the materials evolve from elastics stage to plastic stage.

Figure 4 shows the effect of the concrete strength on the behavior of the SFRCFST specimens. In the linear stage, the slope of the specimens with higher strength concrete is deeper, indicating a higher stiffness. In the elastic-plastic stage, the specimens with higher strength concrete have a smaller axial shortening at the onset of yielding and the ultimate strength. In the softening stage, the decreasing branch of the specimens with higher strength concrete exhibits a deeper slope, and the axial shortening at 85% of the ultimate strength decreases with the increase of the concrete strength. Increasing the concrete strength decreases the deformation capacity and the ductility of the SFRCFST specimens. This is consistent with the results of the PCFST columns [20].

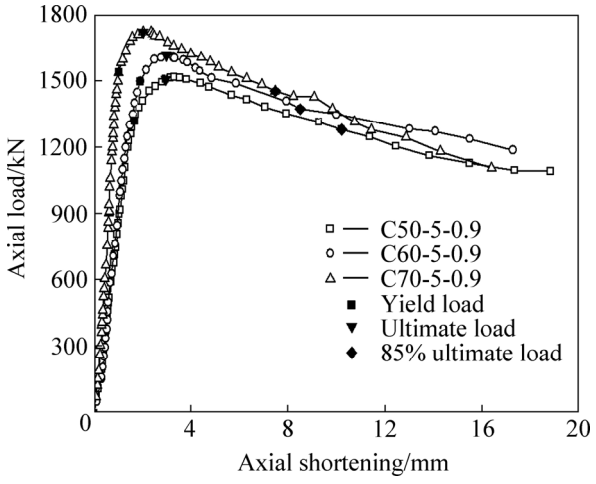

Fig. 4 Comparisons of axial load−axial shortening responses in terms of concrete strength

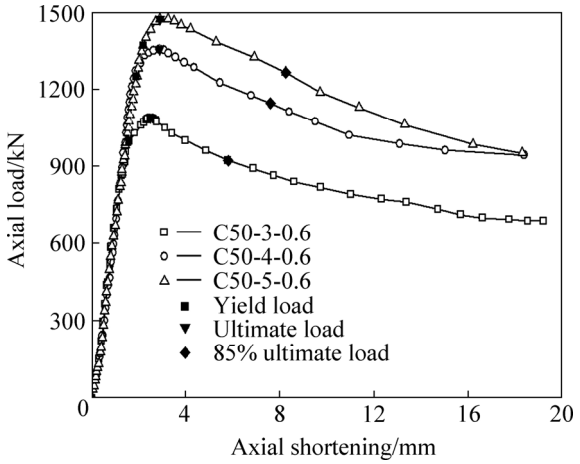

Fig. 5 Comparisons of axial load–axial shortening responses in terms of thickness of steel tube

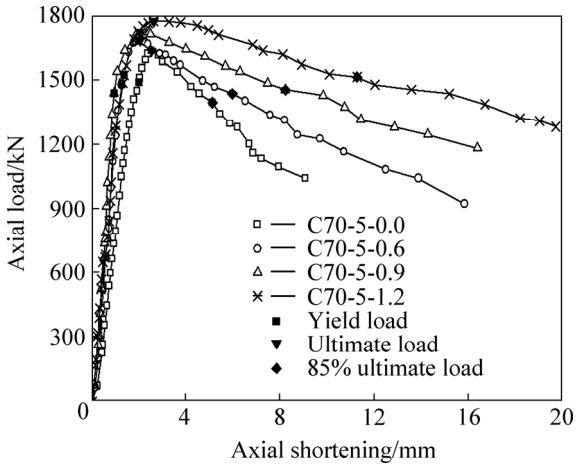

Fig. 6 Comparisons of axial load−axial shortening responses in terms of steel fiber volume fraction

Figure 5 compares the behavior of the SFRCFST specimens with different thicknesses of steel tubes. The specimen with thicker steel tube exhibits a longer linear axial load–axial shoretening response. With the increase of the thickness of steel tube, the axial shortening at 85% of the ultimate strength also increases. Thus, the thickness of steel tube is still one of the sensitive parameters in SFRCFST specimens, which is similar to that of the PCFST columns [21].

The effect of steel fiber is determined by comparing the behavior of the SFRCFST specimens with that of the corresponding PCFST specimens. Figure 6 shows the axial load–axial shortening curves for the specimens of group C70-5. Similar axial load–axial shortening behavior is also found in other groups. The PCFST specimens and SFRCFST specimens exhibit similar axial load–axial shortening curve, in which an ascending branch is followed by a descending branch. Somewhat differently, the slope of the decreasing branches for the SFRCFST specimens is smaller than that for the PCFST specimens, representing an improved post-peak behavior

from the addition of steel fibers. This behavior indicates that adding steel fibers has considerable effect on the ductility and deformation capacity of the CFST columns.

3.3 Energy dissipation capacity

The significant increase of the axial shortening at 85% of the ultimate strength indicates an enhanced energy dissipation capacity. In this work, the energy dissipation capacity E is defined as the dissipated energy when the axial load reduces to 85% of the ultimate strength. The energy dissipation capacity of all specimens is calculated and shown in Table 1. It is apparent that the SFRCFST specimens have a better energy dissipation capacity than the corresponding PCFST specimens. Compared with the corresponding PCFST specimens, the energy dissipation capacity of the SFRCFST specimens with 0.6%, 0.9% and 1.2% steel fibers obtain enhancements of 14.9%–31.7%, 25.3%–94.1% and 85.5%–220.2%, respectively. Thus, the addition of steel fibers can significantly enhance the energy dissipation capacity of the CFST columns.

3.4 Strength index

In order to evaluate the effect of steel fiber reinforced concrete and the local buckling on the load carrying capacity, a strength index (SI, I_s) is defined for the CFST columns as

$$I_s = \frac{N_u}{A_s f_y + A_c f_c'} \tag{1}$$

where N_u is measured ultimate strength; A_s and A_c are the areas of the steel tube and the concrete core, respectively; f_y is the yield strength of steel tube; f_c' is the cylinder strength of concrete (PC and SFRC), and given by $f_c' = 0.8f_{cu}$.

The values of the strength index SI determined are listed in Table 1. These values are correlated with the concrete strength, the thickness of steel tube and the steel fiber volume fraction and range between 1.16 and 1.39.

Generally, the values of the strength index SI increases with the increase of the thickness of steel tube, and decreases when the concrete strength increases. The reasons are that the confining index θ of the specimen, as defined by Eq. (2), increases with the increase of the thickness of steel tube, and decreases with the increase of the concrete strength, i.e. the composite action of the steel tube and the concrete core becomes smaller:

$$\theta = \frac{A_s f_y}{A_c f_c'} \tag{2}$$

The effect of confinement index θ on the strength index SI is shown in Fig. 7. SI shows an obvious increase with the increase of θ when θ is relatively small, but maintains a steady value when θ reaches a level of 0.9. It is worth noting that in the case of the specimens with C50 and C60 concrete, for the specimens of the same group, SI generally increases with the decrease of the confinement index, i.e. when the strength of concrete matrix and the thickness of steel tube are the same, SI increases with increasing the steel fiber volume fraction, but for the specimens with C70 concrete, this phenomenon is not observed until 1.2% steel fibers are added into concrete. It can be inferred from this situation that the addition of steel fibers into concrete may improve the composite action between the steel tube and the concrete core.

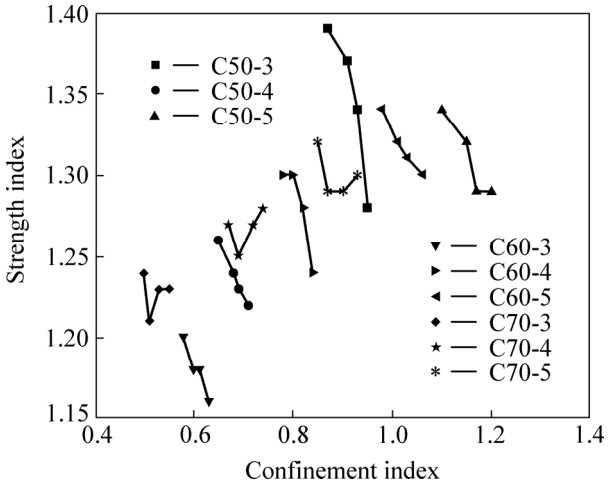

Fig. 7 Strength index versus confinement index

3.5 Ductility

From Fig. 6, different post-peak behaviors between the SFRCFST specimens and the corresponding PCFST specimen can be observed. The slope of the post-peak descending branch is more moderate for the SFRCFST specimens, indicating a better ductile behavior. The δ_{85}/δ_u ratio can be used to evaluate the ductile behavior [22−23]. δ_{85} is the axial shortening at 85% of the ultimate strength in the descending branch of axial load−axial shortening curve, and δ_u is the axial shortening at the ultimate strength. The δ_{85}/δ_u values are shown in Table 1, which are about 2 for the PCFST specimens, and generally larger than 4 for the SFRCFST specimens with 1.2% steel fibers. Thus, it may be concluded that using SFRC as infill in steel tube columns is an effective way to improve their post-peak behavior. In SFRCFST specimens, the presence of steel fibers results in a considerable improvement of the post-cracking response of concrete, then delays the local buckling of steel tube and prevents a sharp decrease of axial load.

The ductility enhancement depends on several parameters, such as the concrete strength, the thickness of steel tube and the steel fiber volume fraction. The methods of adding steel fibers into concrete and using

thicker steel tube are expected to improve the ductility of the CFST columns.

The effect of the thickness of steel tube is determined by comparing the ductility of the PCFST specimens with 3 mm thick steel tube with the ductility of the PCFST specimens with 4 and 5 mm thick steel tube, and by comparing the ductility of the PCFST specimens with 4 mm thick steel tube with the ductility of the PCFST specimens with 5 mm thick steel tube. The ductility enhancements due to the increase of the thickness of steel tube are generally lower than 20%.

The effect of the steel fibers is determined by comparing the ductility of the SFRCFST specimens with that of the corresponding PCFST specimens. Compared with the benchmark PCFST specimens, the SFRCFST columns with 0.6%, 0.9% and 1.2% steel fibers obtain ductility enhancements of 2.0%−47.0%, 33.0%−76.0% and 50.0%−123.0%, respectively. By comparison, the ductility enhancements by the steel fibers are much higher than those obtained from thicker steel tube. From the ductility aspect, adding steel fibers into concrete is a more effective and economical method than using thicker steel tube.

The ductility enhancements analyzed in terms of steel fiber volume fraction, as well as the concrete strength, are shown in Fig. 8. When the steel fiber volume fraction is relatively small, like 0.6%, the efficiency of steel fiber in ductility enhancement is not so high. It is worth noting that the ductility enhancement increases with a higher rate when the steel fiber volume fraction increases. To achieve an effective improvement in the ductility of the high strength concrete filled steel tube columns, a high steel fiber volume fraction, such as 0.9% and 1.2%, may be needed.

It can also be seen from Fig. 8 that the CFST specimens with higher strength concrete obtain higher ductility enhancements. This indicates that steel fibers may be more effective in improving the ductility of the CFST specimens with higher strength concrete. This may be due to the higher interface bond strength between the matrix and steel fiber.

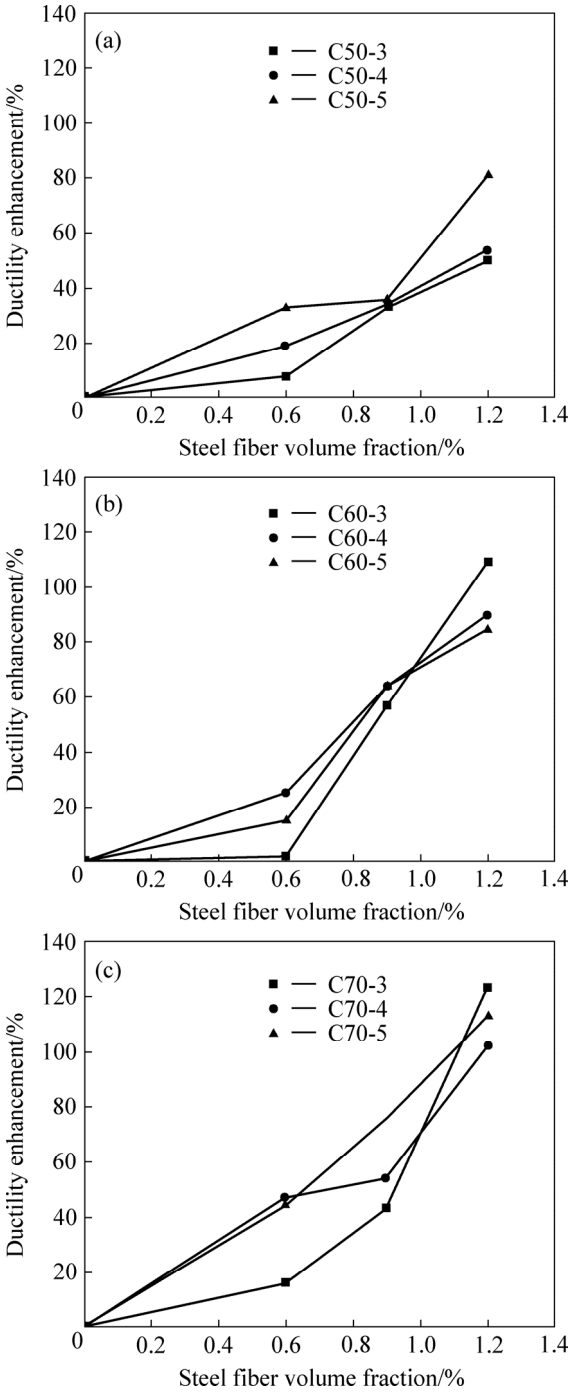

Fig. 8 Influence of volume fraction of steel fiber on ductility enhancement

4 Analytical investigations

In this section, an analytical model is developed to predict the ultimate strength of SFRCFST columns subjected to axial load. For a CFST column, the lateral displacement of the steel tube, due to the higher Poisson ratio, is larger than that of the concrete core in the initial stage of loading, therefore, a separation between the steel tube and the concrete core occurs. As the axial load increases, the Poisson ratio for the concrete increases, and then the lateral displacement of concrete catches up with that of the steel tube at a certain longitudinal strain. As the axial load increases further, transverse stress in the steel tube is developed, and the concrete core is subjected to triaxial compression. When steel fibers are added into concrete, the steel fibers provide additional confinement to the concrete by bridging the cracks. Therefore, the compressive behavior of concrete core is improved, as well as that of the CFST columns. The enhanced behavior of concrete is closely related to the steel fiber volume fraction.

The ultimate strength N_u of a CFST column can be

determined by the following equation:

$$N_u = A_c\sigma_{cc} + A_s\sigma_{sz} \quad (3)$$

where σ_{cc} and σ_{sz} are the strength of confined concrete and the longitudinal stress of steel tube, respectively.

The strength of the confined concrete can be estimated by

$$\sigma_{cc} = f_c' + k\sigma_r \quad (4)$$

where k is the confinement coefficient and equal to 4.1 according to RICHART et al [24], and σ_r is the confining pressure.

The biaxial stresses in the steel tube at the ultimate strength are

$$\sigma_{s\theta} = \alpha f_y \quad (5)$$

$$\sigma_{sz} = \beta f_y \quad (6)$$

where $\sigma_{s\theta}$ and σ_{sz} are the transverse stress and the longitudinal stress in the steel tube, respectively; α and β are the coefficients determined based on the test results.

The confining pressure σ_r provided by the steel tube can be calculated by using the following equation:

$$\sigma_r = -\frac{2t}{D-2t}\sigma_{s\theta} \quad (7)$$

To evaluate the confining effect on concrete strength, it is assumed that the difference between the ultimate strength N_u and the nominal squash load N_0 is provided by the confining effect on concrete strength. The difference can be estimated as a linear function of the tube yield strength N_s for PCFST columns through an augmentation factor [1]. In SFRCFST columns, the confinements provided by the steel fibers and the steel tube both contribute to the strength gain. To take into account the confinement effect of steel fibers, the augmentation factor is expressed as a function of V_f and determined on the test results. Thus, the strength gain can be interpreted as follows:

$$N_u - N_0 = \lambda(V_f)N_s \quad (8)$$

$$\frac{N_u}{N_0} = 1 + \lambda(V_f)\frac{N_s}{N_0} \quad (9)$$

where N_0 and N_s can be estimated by Eqs. (10) and (11), respectively:

$$N_0 = A_s f_y + A_c f_c' \quad (10)$$

$$N_s = A_s f_y \quad (11)$$

From Eqs. (3)–(11), the factor λ is given by

$$\lambda(V_f) = \frac{N_u - N_0}{N_s} = \beta - 1 - \frac{D-2t}{2(D-t)}k\alpha \quad (12)$$

The calculated values of λ are listed in Table 1. The values of λ increase with the increase of steel fiber volume fraction. The expression for $\lambda(V_f)$ can be obtained by linear regression, as shown in Fig. 9, and can be expressed by

$$\lambda(V_f) = 0.55 + 19V_f \quad (13)$$

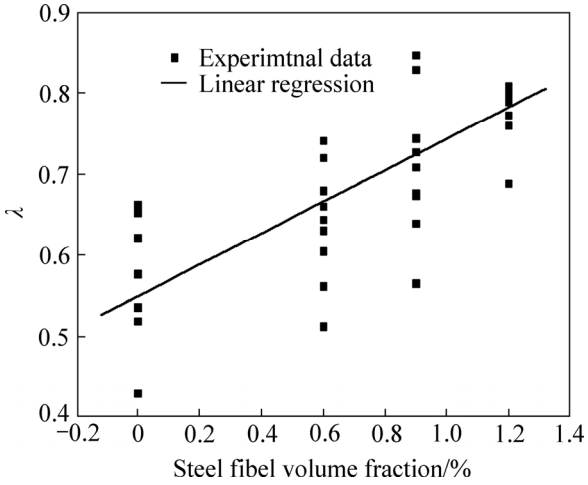

Fig. 9 Relationship between λ and steel fiber volume fraction

Assume that steel stresses at the ultimate state given by Eqs. (5) and (6) satisfy the von Mises yield criterion given by

$$\sigma_{s\theta}^2 - \sigma_{s\theta}\sigma_{sz} + \sigma_{sz}^2 = f_y^2 \quad (14)$$

Thus, the relationship between α and β can be determined by substituting Eqs. (5) and (6) into Eq. (14):

$$\alpha^2 - \alpha\beta + \beta^2 = 1.0 \quad (15)$$

From Eqs. (12), (13) and (15), stress coefficients α and β can be calculated by Eqs. (16) and (17), respectively:

$$\alpha = \frac{-4.65 - 57V_f + \sqrt{-1100V_f^2 - 178V_f + 4.2}}{6} \quad (16)$$

$$\beta = \frac{\sqrt{-1100V_f^2 - 178V_f + 4.2}}{3} \quad (17)$$

The values of α and β determined by Eqs. (16) and (17), respectively, are shown in Fig. 10. With the increase of steel fiber volume fraction, the absolute value of α increases, while β decreases. From Eqs. (5) and (6), the transverse stress of the steel tube increases and the longitudinal stress decreases when the steel fiber volume fraction increases. This indicates that the steel tube can provide a higher level of lateral pressure when steel fiber reinforced concrete is used as infill.

In this model, the strength of the corresponding plain concrete is used to predict the ultimate strength of the SFRCFST columns. The comparisons of the experimental results N_u in this work and the predictions

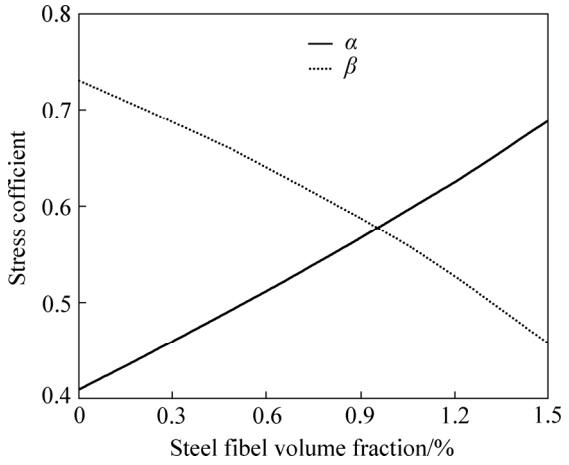

Fig. 10 Revolution of α and β with steel fiber volume fraction

N_c are shown in Table 1 and Fig. 11. A mean ratio (N_u/N_c) of 0.99 with a standard deviation of 0.035 is obtained.

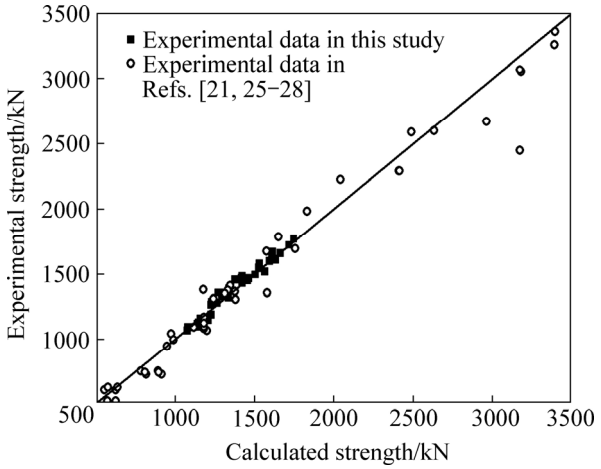

Fig. 11 Comparison of strength between experimental results and predictions

To evaluate the accuracy of the predicting model, the experimental results of the PCFST columns reported in Refs. [21, 25−28] are also compared with the predicted results. The comparisons are shown in Fig. 11. As can be seen, the predictions are reasonable for the experimental results. A mean ratio (N_u/N_c) of 1.03 with a standard deviation of 0.101 is obtained.

5 Conclusions

1) Adding steel fibers into concrete can significantly improve the ductility and the energy dissipation capacity of the CFST columns, but has no obvious effect on the ultimate strength and the failure mode.

2) Adding steel fibers into concrete is more effective than using thicker steel tube in improving the post-peak behavior of the CFST columns. And the effect of steel fiber is more pronounced for the columns with higher strength concrete.

3) The transverse stress of the steel tube increases, while the longitudinal stress decreases at the ultimate strength when the steel fiber volume fraction increases.

4) A simple model is proposed to calculate the ultimate strength of the CFST columns. The predicted results are in good agreement with the experimental ones obtained in this work and in the literature.

References

[1] SAKINO K, NAKAHARA H, MORINO S, NISHIYAMA A. Behavior of centrally loaded concrete-filled steel tube short columns [J]. Journal of Structural Engineering ASCE, 2004, 130(2): 180−188.

[2] GOURLEY B C, TORT C, DENAVIT M D, SCHILLER P H, HAJJAR J F. A synopsis of studies of the monotonic and cyclic behavior of concrete-filled steel tube beam-columns [R]. Urbana, US: Department of Civil and Environmental Engineering, University of Illinois at Urbana-Champaign, 2008.

[3] LIU Da-lin, GHO W M. Axial load behaviour of high-strength rectangular concrete-filled steel tubular stub columns [J]. Thin-Walled Structures, 2005, 43(8): 1131−1142.

[4] ZEGHICHE J, CHAOUI K. An experimental behaviour of concrete-filled steel tubular columns [J]. Journal of Constructional Steel Research, 2005, 61(1): 53−66.

[5] FUJIMOTO T, MUKAI A, NISHIYAMA I, SAKINO K. Behavior of eccentrically loaded concrete-filled steel tubular columns [J]. Journal of Structural Engineering, 2004, 130(2): 203−212.

[6] ZHANG Su-mei, WANG Yu-yin. Failure modes of short columns of high-strength concrete-filled steel tubes [J]. China Civil Engineering Journal, 2004, 37(9): 1−10. (in Chinese)

[7] TAO Zhong, HAN Lin-hai, WANG Dong-ye. Strength and ductility of stiffened thin-walled hollow steel structural stub columns filled with concrete [J]. Thin-Walled Structures, 2008, 10(46): 1113−1128.

[8] CHEN Xiang-yu, DING Yi-ning, AZEVEDO C. Combined effect of steel fibres and steel rebars on impact resistance of high performance concrete [J]. Journal of Central South University of Technology, 2011, 18(5): 1677−1684.

[9] CAMPIONE G, MINDESS S, SCIBILIA N, ZINGONE G. Strength of hollow circular steel sections filled with fibre-reinforced concrete [J]. Canadian Journal of Civil Engineering, 2000, 27: 364−372.

[10] CAMPIONE G, MENDOLA L L, SANPAOLESI L, SCIBILIA N, ZINGONE G. Behavior of fiber reinforced concrete-filled tubular columns in compression [J]. Materials and Structures, 2002, 35: 332−337.

[11] ELLOBODY E, GHAZY M F. Experimental investigation of eccentrically loaded fibre reinforced concrete-filled stainless steel tubular columns [J]. Journal of Constructional Steel Research, 2012, 76: 167−176.

[12] ELLOBODY E, GHAZY M F. Polypropylene fiber reinforced concrete-stainless steel composite columns: Design and behavior [J]. Advances in Structural Engineering, 2013, 16(3): 427−440.

[13] TAO Zhong, UY B, HAN Lin-hai, WANG Zhi-bin. Analysis and design of concrete-filled stiffened thin-walled steel tubular columns under axial compression [J]. Thin-Walled Structures, 2009, 47(12): 1544−1556.

[14] GOPAL S R, MANOHARAN P D. Tests on fibre reinforced concrete filled steel tubular columns [J]. Steel and Composite Structures, 2004, 4: 37−48.

[15] KODUR V K R, LIE T T. Fire resistance of circular steel columns filled with steel fiber-reinforced concrete [J]. Journal of Structural Engineering, 1996, 122(7): 776−782.

[16] TOKGOZ S, DUNDAR C. Experimental study on steel tubular

columns in-filled with plain and steel fiber reinforced concrete [J]. Thin-Walled Structures, 2010, 48(6): 414−422.

[17] PORTOLES J M, SERRA E, ROMERO M L. Influence of ultra-high strength infill in slender concrete-filled steel tubular columns [J]. Journal of Constructional Steel Research, 2013, 86: 107−114.

[18] LIEW J Y R, XIONG D X. Ultra-high strength concrete filled composite columns for multi-story building construction [J]. Advances in Structural Engineering, 2012, 15(9): 1487−1503.

[19] de OLIVEIRA W L A, de NARDIN S, el DEBS A L H C, el DEBS M K. Influence of concrete strength and length/diameter on the axial capacity of CFT columns [J]. Journal of Constructional Steel Research, 2009, 65(12): 2103−2110.

[20] ELLOBODY E, YOUNG B, LAM D. Behaviour of normal and high strength concrete-filled compact steel tube circular stub columns [J]. Journal of Constructional Steel Research, 2006, 62(7): 706−715.

[21] ABED F, ALHAMAYDEH M, ABDALLA S. Experimental and numerical investigations of the compressive behavior of concrete filled steel tubes (CFSTs) [J]. Journal of Constructional Steel Research, 2013, 80: 429−439.

[22] HAN Lin-hai. Tests on stub columns of concrete-filled RHS sections [J]. Journal of Constructional Steel Research, 2002, 58(3): 353−372.

[23] TAO Zhong, HAN Lin-han, WANG Zhi-bin. Experimental behaviour of stiffened concrete-filled thin-walled hollow steel structural (HSS) stub columns [J]. Journal of Constructional Steel Research, 2005, 61(7): 962−983.

[24] RICHART F E, BRANDZAEG A, BROWN R L. The failure of plain and spirally reinforced concrete in compression [R]. Urbana, US: Univ. Illinois, Engineering Experimental Station, 1929.

[25] GIAKOUMELIS G, LAM D. Axial capacity of circular concrete-filled tube columns [J]. Journal of Constructional Steel Research, 2004, 60(7): 1049−1068.

[26] GUPTA P K, SARDA S M, KUMAR M S. Experimental and computational study of concrete filled steel tubular columns under axial loads [J]. Journal of Constructional Steel Research, 2007, 63(2): 182−193.

[27] O'SHEA M D, BRIDGE R Q. Design of circular thin-walled concrete filled steel tubes [J]. Journal of Structural Engineering, 2000, 126(11): 1295−1303.

[28] YU Qing, TAO Zhong, WU Ying-xing. Experimental behaviour of high performance concrete-filled steel tubular columns [J]. Thin-Walled Structures, 2008, 46(4): 362−370.

(Edited by FANG Jing-hua)